Implications of different ocean color products in a global ocean model: Sensitivity analyses for NINO3.4 region

Hae-Cheol Kim[1,*], Avichal Mehra[2], Sudhir Nadiga[1], Zulema Garraffo[1], Seunghyun Son[3], Eric Bayler[4]
[1]IMSG at NWS/NCEP/EMC, [2]NWS/NCEP/EMC, [3]CIRA at NESDIS, [4]NESDIS
Email: Hae-Cheol.Kim@noaa.gov; Phone: 301-683-3700

This is a study funded by Joint Polar Satellite System (JPSS) - Proving Ground and Risk Reduction (PGRR) Program at NOAA's National Environmental Satellite, Data, and Information Service (NESDIS). The main motivation of this study is to demonstrate how various ocean color products can be used in a global ocean modeling framework [1], and to investigate effects of different combinations of atmospheric forcings (Climate Forecasting System Reanalysis (CFSR) [2]; Reanalysis 2 (RA2) [3]) and ocean color products on the upper water thermal structure of the NINO3.4 region (5°N - 5°S and 170°W - 120°W).

Two ocean color (OC) products (Sea-Viewing Wide Field-of-View Sensor (SeaWiFS); Visible Infrared Imager Radiometer Suite (VIIRS)) and two different optical algorithms for computed short-wave radiant fluxes [4][5] are used for computing shortwave radiant fluxes in water, and they were combined with two different atmospheric forcings (CFSR and RA2) for creating eleven numerical experiments of a global ocean model (Table 1). Effects of different optical parameterizations and frequencies of ocean color products along with different forcings on the upper ocean thermal structure are then quantitatively compared.

Table 1. Various ocean color products and temporal frequencies used for computing short wave radiant fluxes combined with different atmospheric forcings in a global ocean modeling framework (H: hourly data used; D: daily-averaged data used; SH; simulated hourly data used for shortwave radiant fluxes only; SZA: solar zenith angle).

Experiments	Ocean color product	Sensor	Forcings	OC Period	Algorithms
KparCLM	Long-term climatological K_{dPAR} [6]	SeaWiFS	CFSR (H)	1997-2010	[4]
ChlaCLM	Long-term climatological Chl-*a* [7]	SeaWiFS	CFSR (H)	1997-2010	[5]
ChlaIND	Interannual mean Chl-*a* [7]	SeaWiFS	CFSR (H)	Each year (2001 – 2010)	[5] No diurnal SZA in water
ChlaID	Interannual mean Chl-*a* [7]	SeaWiFS	CFSR (H)	Each year (2001 – 2010)	[5] Diurnal SZA in water
KparSWFclmD	Long-term climatological K_{dPAR} [6]	SeaWiFS	RA2 (D)	1997-2010	[4]
KparVRSclmD	Long-term climatological K_{dPAR} [6]	VIIRS	RA2 (D)	2012-2015	[4]
KparVRSclmH	Long-term climatological K_{dPAR} [6]	VIIRS	RA2 (SH)	2012-2015	[4]
ChlaSWFclmD	Long-term climatological Chl-*a* [7]	SeaWiFS	RA2 (D)	1997-2010	[5] No diurnal SZA in water
ChlaVRSclmD	Long-term climatological Chl-*a* [7]	VIIRS	RA2 (D)	2012-2015	[5] No diurnal SZA in water
ChlaVRSclmH	Long-term climatological Chl-*a* [7]	VIIRS	RA2 (SH)	2012-2015	[5] No diurnal SZA in water
ChlaVRSclmDW	Long-term climatological Chl-*a* [7]	VIIRS	RA2 (D)	2012-2015	[5] Diurnal SZA in water

Hybrid Coordinate Ocean Model (HYCOM; GLBa0.24 hereafter) with cylindrical (78.64°S – 66°S); recti-linear coordinate (66°S – 47°N); and. Arctic bipolar patch (>47°N) is used. HYCOM has vertical coordinates employing 32 layers with following isopycnals in the deep sea, z-levels in the surface and terrain-following σ-coordinate near coastal areas [1]. K-Profile Parameterization (KPP) [8] is used as a vertical mixing scheme. GLBa0.24 is forced by either hourly atmospheric fluxes from NOAA's CFSR [2] or daily averaged RA2 [3]. Temperature averaged over the upper 100m at the NINO3.4 region is selected to quantify the impact of each numerical runs, and Global Ocean Data Assimilation System (GODAS) [9] is used for verification purposes.

All experiments are divided into two large groups: SeaWiFS-CFSR (red fonts in Table 1) and VIIRS-RA2 combination (blue fonts in Table 2), respectively. The first four numerical experiments in Table 1 (KparCLM; ChlaCLM; ChlaIND; and ChlaID) belong to SeaWiFS-CFSR combination, where, the last seven experiments (KparSWFclmD; KparVRSclmD; KparVRSclmH; ChlaSWFclmD; ChlaVRSclmD; ChlaVRSclmH; and ChlaVRSclmDW) are from the second group. Simulation period for the first group is 2001-2009 and for the second group is 2012-2015, respectively.

In summary, the comparison of the first group against GODAS product reveals that algorithmic differences (KparCLM versus ChlaCLM, ChlaIND, ChlaND) are noticeable, and that KparCLM yields better results with respect to root mean squared difference (RMSD) and correlation (Fig. 1a). Comparisons between the members in the second group and GODAS indicate that neither ocean color products nor algorithms used for shortwave radiation seem to have much impact (Fig. 1b) in improving simulated results or changing the thermal structure. However, it should be noted that temporal frequency of shortwave radiant fluxes (simulated hourly versus daily) makes noticeable differences in the top 100m averaged temperatures of the NINO3.4 region (Fig. 1b).

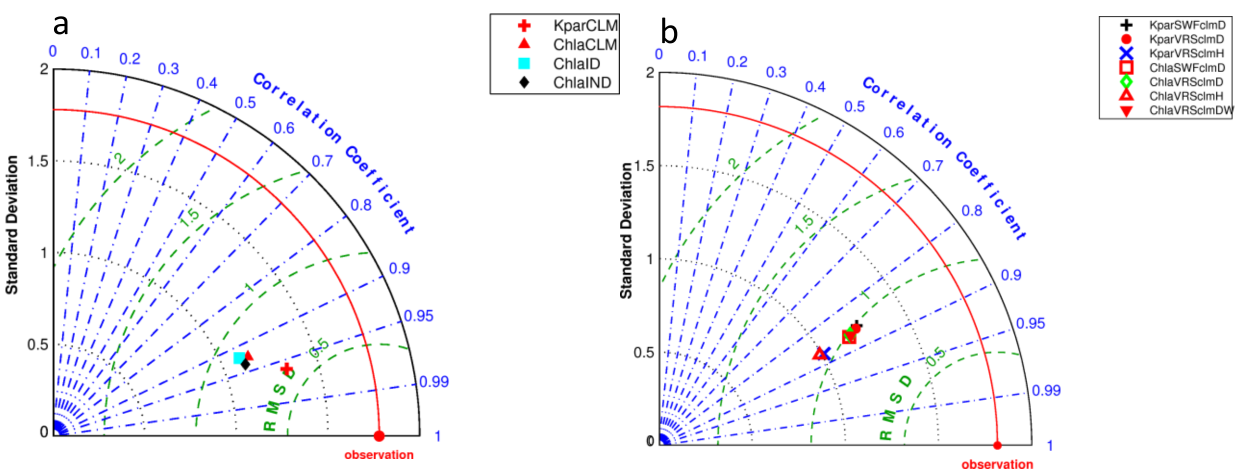

Fig. 1. Taylor diagrams for comparisons of all numerical experiments against GODAS. Comparisons between members of the first group (a) and the second group (b) with GODAS are presented, respectively.

[1] Bleck, R., 2002: An oceanic general circulation model framed in hybrid isopycnic-Cartesian coordinates, Ocean Model., 37, 55-88.
[2] Saha, S., *et al.* (2010) The NCEP climate forecast system reanalysis. Bull. Amer. Meteor. Soc., 91, 1015–1057.
[3] Kanamitsu, M., W. Ebisuzaki, J. Woollen, S Yang, J. Hnilo, M. Fiorno, and G. Potter (2002) NCEP-DOE. AMIP-II Reanalysis (R-2). Bull. Amer. Meteor. Soc., 83, 1631-1643.
[4] Kara, A.B., H.E. Hurlburt, P.A. Rochford, and J.J. O'Brien (2004). The impact of water turbidity of the interannual sea surface temperature simulations in a layered global ocean model. J. Phys. Oceanogr., 34, 345–359.
[5] Lee, J., K. Du, R. Arnone, S. Liew, and B. Penta (2005), Penetration of solar radiation in the upper ocean: A numerical model for oceanic and coastal waters, J. Geophys. Res., 110, 1-12.
[6] Son, S. and M. Wang (2015) Diffuse attenuation coefficient of the photosynthetically available radiation Kd(PAR) for global open ocean and coastal waters, Remote Sens. of Environ., 159, 250-258.
[7] O'Reilly, J.E., S. Maritorena, B.G. Mitchell, D.A. Siegel, K L. Carder, S. A. Garver, M. Kahru, and C. McClain (1998), Ocean color chlorophyll algorithms for SeaWiFS, J. Geophys. Res., 103, 24,937-24,954.
[8] Large, W.C., J.C. McWilliams and S.C. Doney, 1994: Oceanic vertical ixing: a review and a model wit a nonlocal boundary layer parameterization. Rev. Geophys. 32, 363-403.
[9] Behringer, D. W., and Y. Xue (2004) Evaluation of the global ocean data assimilation system at NCEP: The Pacific Ocean. Eighth Symposium on Integrated Observing and Assimilation Systems for Atmosphere, Oceans, and Land Surface, AMS 84th Annual Meeting, Washington State Convention and Trade Center, Seattle, Washington, 11-15.